Journal of Integrative Neuroscience

J. Integr. Neurosci. **2026**; 25(8): 46741
https://doi.org/10.31083/JIN46741

Original Research

Gamma and Beta Neurofeedback Training Can Improve Visual Perception With Spectral and Regional Specificity

Lu Wang[1], Yong Wang[2], Zhaohuan Ding[3], He Chen[4,5,*], Xiaoli Li[1,4,5,*]

[1]State Key Laboratory of Cognitive Neuroscience and Learning & IDG/McGovern Institute for Brain Research, Beijing Normal University, 100875 Beijing, China
[2]Department of Rehabilitation Medicine, Zhujiang Hospital, Southern Medical University, 510280 Guangzhou, Guangdong, China
[3]Shien-Ming Wu School of Intelligent Engineering, South China University of Technology, 510640 Guangzhou, Guangdong, China
[4]School of Automation Science and Engineering, South China University of Technology, 510641 Guangzhou, Guangdong, China
[5]Guangdong Artificial Intelligence and Digital Economy Laboratory (Guangzhou), 510335 Guangzhou, Guangdong, China
*Correspondence: chenhe@scut.edu.cn (He Chen); xiaoli@bnu.edu.cn (Xiaoli Li)
Academic Editor: Bettina Platt
Submitted: 19 September 2025 Revised: 5 April 2026 Accepted: 29 May 2026 Published: 26 August 2026

Abstract

Background: Gamma and beta oscillations of electroencephalography (EEG) are involved in multiple perceptual information processing. Neurofeedback training (NFB) is a non-invasive neuromodulation approach that provides an endogenous paradigm to investigate the causal relationship between brain oscillations and cognitive abilities. In this study we investigated the effectiveness and specificity of gamma and combined gamma-beta NFB training for improving visual perception in healthy adults. **Methods:** A total of 48 healthy participants were recruited and randomly assigned into three groups. Four participants withdrew during the study, leaving 44 participants for final analysis : a sham group (n = 14), a gamma NFB training group (n = 16) targeting parieto-occipital (PO) gamma rhythms, and a gamma-beta training group (n = 14) targeting both PO gamma and central beta rhythms. All participants underwent six NFB sessions, each containing nine blocks. Baseline tasks for resting state and visual perception measurements were conducted before and after NFB training. **Results:** Both training groups showed significant improvements in reaction time and accuracy. Importantly, EEG data obtained during the training process and baseline tests showed that relative PO gamma rhythms were increased in both groups, while relative central beta rhythms were enhanced only in the gamma-beta group. EZ-diffusion model analysis revealed that these improvements were primarily driven by increased drift rates and reduced non-decision times, suggesting enhanced efficiency in perceptual evidence accumulation. **Conclusions:** The current results validate the effectiveness of NFB training and demonstrate clear spectral and regional specificity, revealing different functional contributions of the two oscillations during visual perception. In the context of a randomized, sham-controlled design, these results provide preliminary causal evidence for the involvement of gamma- and beta-band activity in visual processing. **Clinical Trial Registration:** No: ChiCTR2600124537. https://www.chictr.org.cn/showproj.html?proj=292703.

Keywords: neurofeedback; electroencephalography; neural oscillations; gamma rhythm; beta rhythm; visual perception; non-invasive neural modulation

1. Introduction

Neural oscillations within electroencephalography (EEG) are a characteristic manifestation of brain activity and play a crucial role across multiple stages of visual perception. Recent studies have provided strong evidence that brain rhythms encode, transmit, and integrate visual information through synchronized oscillatory activities of neuronal populations [1,2]. Extensive studies have indicated that beta oscillations are closely associated with arousal states, including vigilance, attention, excitement, and cognitive processes [3,4]. Gamma oscillations are mostly involved with the local cortical processing of information, such as sensory and perceptual information [5].

Perceptual processing mainly involves two stages: the receiving and processing of sensory inputs, and the subsequent integration of sensory information. The former occurs mainly in the primary visual and auditory cortices for feature encoding, and predominantly involves gamma and high-gamma oscillations. The latter occurs in higher-order cortical regions that integrate diverse sensory inputs [6,7,8,9,10], and primarily involves relatively slower oscillations. Therefore, gamma and beta rhythms may contribute differently to the visual perception process, but their causal roles remain to be investigated.

To transition from correlation to causality, it is essential to experimentally manipulate neural rhythms and assess the subsequent behavioral consequences [11,12]. Non-invasive exogenous brain stimulation techniques, including transcranial electrical stimulation (tES) and transcranial magnetic stimulation (TMS), provide an avenue for such manipulation. However, such methods rely on exogenous currents that passively entrain brain activity [13,14,15]. These exogenous modulatory methods typically have limited spectral selectivity, often affect relatively large cortical territories, and may induce non-specific side-effects or discomfort [15,16,17,18,19]. In contrast, neurofeed-

back (NFB) provides a unique advantage by enabling endogenous neuromodulation [3,20,21,22]. By training participants to voluntarily self-modulate specific frequency bands and then subsequently examining changes in performance, NFB allows researchers to disentangle the direct functional contribution of specific oscillations to behavior [23,24,25,26,27]. Consequently, NFB is ideally suited to test the hypothesis that enhancing gamma or beta activity causally improves distinct stages of visual perception.

NFB training enables endogenous regulation of neural activity via closed-loop operant conditioning [3,21]. Unlike exogenous stimulation methods that passively entrain brain rhythms, NFB leverages the brain's intrinsic plasticity to achieve frequency and region modulation [21,28]. NFB is therefore a critical methodological tool that has been widely used to modulate various behavior-related functional networks [29,30,31,32], and provides an alternative self-administered therapy [33,34,35]. Furthermore, it allows causal inference between brain activity and behavior, and can verify the causal contributions of specific neural rhythms to visual perception [29].

In recent preliminary studies, gamma and beta NFB training showed efficacy for enhancing visual perception. Gamma-enhancement NFB training was found to improve perceptual binding capabilities [36], with participants in the training group exhibiting faster perceptual processing speed compared to the control group [24]. NFB that targets beta has been reported to significantly improve visual information processing [37]. Moreover, increasing the bioelectrical activity within the electroencephalography (EEG) beta band has been associated with enhanced oriented visual perception during task execution [38]. The effects of beta-strengthening NFB protocols on visuomotor performance have also been investigated in athletes. The results showed reduced visual reaction time in both simple and complex tasks, suggesting an improvement in the speed and efficiency of visual processing [39]. These findings demonstrate that NFB can, in principle, be used to modulate oscillatory activity in functionally meaningful ways.

However, such positive results do not by themselves establish that the behavioral benefits are spectrally and regionally specific to the trained rhythm and cortical site. Conventional single-frequency, single-electrode protocols implicitly assume that NFB selectively modifies the targeted band while leaving non-target bands unchanged, and that the feedback electrode mainly reflects activity from the underlying cortical region [40,41,42,43]. Empirical work challenges both assumptions, since increases in the trained band are frequently accompanied by concomitant changes in other frequency bands ("band non-specificity"), and scalp EEG at a single electrode reflects a linear mixture of multiple spatially distributed sources due to volume conduction. Therefore, existing single-band, single-site studies cannot unambiguously attribute behavioral changes to a spectrally and regionally circumscribed neural substrate. The results of a rare study that combined scalp and intracranial recordings during gamma-NFB in epilepsy patients further suggest that training can modulate gamma power across both local and more distributed sites [44]. This reinforces the notion that NFB acts at the network level rather than on an isolated cortical patch. However, without verifying spectral specificity, it is difficult to distinguish precise neuromodulation from generalized non-specific effects.

As outlined above, perceptual processing depends on the coordination between local feature encoding in early sensory cortices, predominantly supported by gamma and high-gamma oscillations, and subsequent large-scale integration across higher-order regions. The latter is more strongly associated with slower rhythms in the beta range [45]. The lack of information regarding potential interactions (e.g., cross-frequency coupling) limits our understanding of how NFB reconfigures the holistic functional architecture of the visual system. Consequently, an NFB approach that jointly considers gamma and beta activity is better positioned to probe not only the causal contribution of each rhythm to distinct stages of visual perception, but also their potential synergistic interactions within the visual processing hierarchy.

To address these issues, the current study compared gamma and gamma-beta NFB training for improving visual perception ability by analyzing behavioral and neurophysiological effects. Our aim was to systematically investigate the specificity of gamma rhythm modulation and potential cross-frequency synergistic mechanisms, thus providing a new framework to understand the functional specificity of neural oscillations and optimize cognitive enhancement strategies.

2. Materials and Methods

2.1 Participants

An a priori power analysis was conducted using G*Power 3.1.9.7 (Heinrich Heine University Düsseldorf, Düsseldorf, Germany) to estimate the required sample size. The calculation was based on a repeated-measures analysis of variance (ANOVA) with a within–between interaction for three groups and two measurement time points. Assuming a medium effect size (Cohen's $f = 0.25$), $\alpha = 0.05$, statistical power $(1 - \beta) = 0.80$, a correlation of 0.50 between repeated measurements, and a nonsphericity correction of $\varepsilon = 1.0$, the analysis indicated a minimum required sample size of 42 participants (approximately 14 per group).

A total of 48 healthy adult participants were recruited for this study from the local university community. All participants were undergraduate or graduate students, with normal or corrected-to-normal vision and no color-vision deficiencies. Participants were randomly assigned to one of three groups, during the study, two participants in the sham group and two participants in the gamma-beta group withdrew for personal reasons related to the time commitment required for the study and did not complete the post-

training visual perception assessment. Consequently, 44 participants (22 females; 21.04 ± 2.16 years [mean ± standard deviation (SD)]) completed the full experimental protocol and were included in the final analysis: sham (n = 14; 7 females; age: 21.20 ± 2.81 years), gamma group (n = 16; 8 females; age: 21.13 ± 1.89 years), and gamma–beta group (n = 14; 7 females; age: 20.79 ± 1.81 years). None of the participants reported neurological or psychiatric disorders, ongoing medication use, or prior involvement in cognitive or behavioral interventions. The participant recruitment, randomization, allocation, follow-up, and final analysis procedures are summarized in the CONSORT 2025 flow diagram (**Supplementary Fig. 1**).

2.2 Experiments

The study employed a double-blind design. Participants were randomly assigned to the sham, gamma, or gamma–beta groups using a computer-generated randomization sequence. This was performed by an experimenter who was not involved in data collection or analysis. The participants and researchers who conducted the NFB and behavioral testing were blinded to group assignment throughout the study, in accordance with the double-blind design.

As shown in Fig. 1a, all participants underwent a visual perception task before and after the NFB training process. This was conducted over 6 consecutive days. Each NFB session contained one block for measuring the resting baseline and 9 blocks for active enhancement of the target rhythms. The experiment was presented on a 24-inch Philips 241V8LB/27 LCD monitor (Philips, Amsterdam, the Netherlands) set to a resolution of 1920 × 1080 pixels and a refresh rate of 100 Hz. Participants were seated 70 cm from the monitor under comfortable viewing conditions.

2.2.1 The Visual Perception Task

As shown in Fig. 1b, a total of 100 animal images and 100 non-animal images were collected from the China Image Set (CIS). CIS is a normative database consisting of 551 high-quality colored stimulus photos with a standardized resolution of 500 × 500 pixels, specifically developed for Chinese speakers [46]. Based on the visual complexity score of CIS, which uses a 5-point Likert scale to reflect the complexity of visual textures and lines, 100 images with closely matched visual complexity were selected from both animal and non-animal pictures. These images were processed using two-dimensional Fourier transformation and phase randomization, and then converted back as stimulus materials. This method preserved the global spatial frequency profiles of the images while disrupting their content, thereby altering the visual content without affecting the physical luminance and amplitude. The task comprised 200 trials in total. As shown in Fig. 1b, in each trial, a distorted image was presented for 200 ms. Participants were instructed to respond as quickly as possible within 1000 ms by pressing the letter ‘F’ or ‘J’ (counterbalanced across participants) to indicate whether the image depicted an animal. A blank screen (600–700 ms) followed each response.

For the visual perception task, continuous EEG data were recorded using a SynAmps 2 system (Compumedics NeuroScan, Charlotte, NC, USA) at a sampling rate of 1000 Hz with 24-bit resolution. A total of 64 active silver/silver chloride (Ag/AgCl) electrodes were placed according to the international 10–20 system, with all scalp electrodes referenced to the Cz electrode during data collection. Specifically, the impedance of all electrodes was kept below 10 kΩ. Offline EEG data processing was performed using the EEGLAB toolbox (v 2022.0; Swartz Center for Computational Neuroscience, University of California San Diego, La Jolla, CA, USA) and custom MATLAB scripts (R2023b; MathWorks Inc, Natick, MA, USA). The data were resampled to 500 Hz, and the notch filter at 50 Hz was applied to eliminate line noise. A zero-phase bandpass filter (0.1–80 Hz, infinite impulse response (IIR)) was applied using the MATLAB filtfilt function. Noise-contaminated electrodes were selected by visual inspection and interpolated via spherical spline interpolation, with the data re-referenced to the average of all scalp electrodes. Independent Component Analysis (ICA) was applied to detect and remove artifacts related to eye blinks, saccades, and muscle activity using the plugin ICLabel. Finally, data were epoched from –200–800 ms after target onset for subsequent analysis. Epochs with muscle activity exceeding ± 80 μV were excluded.

2.2.2 Neurofeedback Sessions

Participants were randomly assigned to one of three NFB protocols. In the sham condition, feedback reflected the relative power spectrum within a randomly selected 4-Hz window (4–48 Hz) at Cz, unrelated to the targeted bands. In the gamma condition, participants were trained to increase gamma-band (30–48 Hz) activity at O1 and O2 channels. In the gamma–beta condition, participants were trained to increase gamma-band (30–48 Hz) at O1 and O2 channels and beta-band (13–30 Hz) at the Cz channel. During the NFB training process, EEG was referenced to bilateral mastoid electrodes (M1, M2), with the impedance of all electrodes maintained below 10 kΩ and a sampling frequency of 1000 Hz.

Each participant was required to undergo six consecutive days of training. The daily training session comprised a 2-minute resting baseline recording, followed by 9 training blocks. Each block lasted 3 minutes, with 30-second resting intervals between blocks. At the onset of each block, the visual feedback interface was reset to its initial size and orientation.

For each session, participants initially sat quietly in front of the screen, and 2-minute eyes-open resting baseline EEG data were recorded while the bar graphs on both sides of the screen remained static and the feedback window

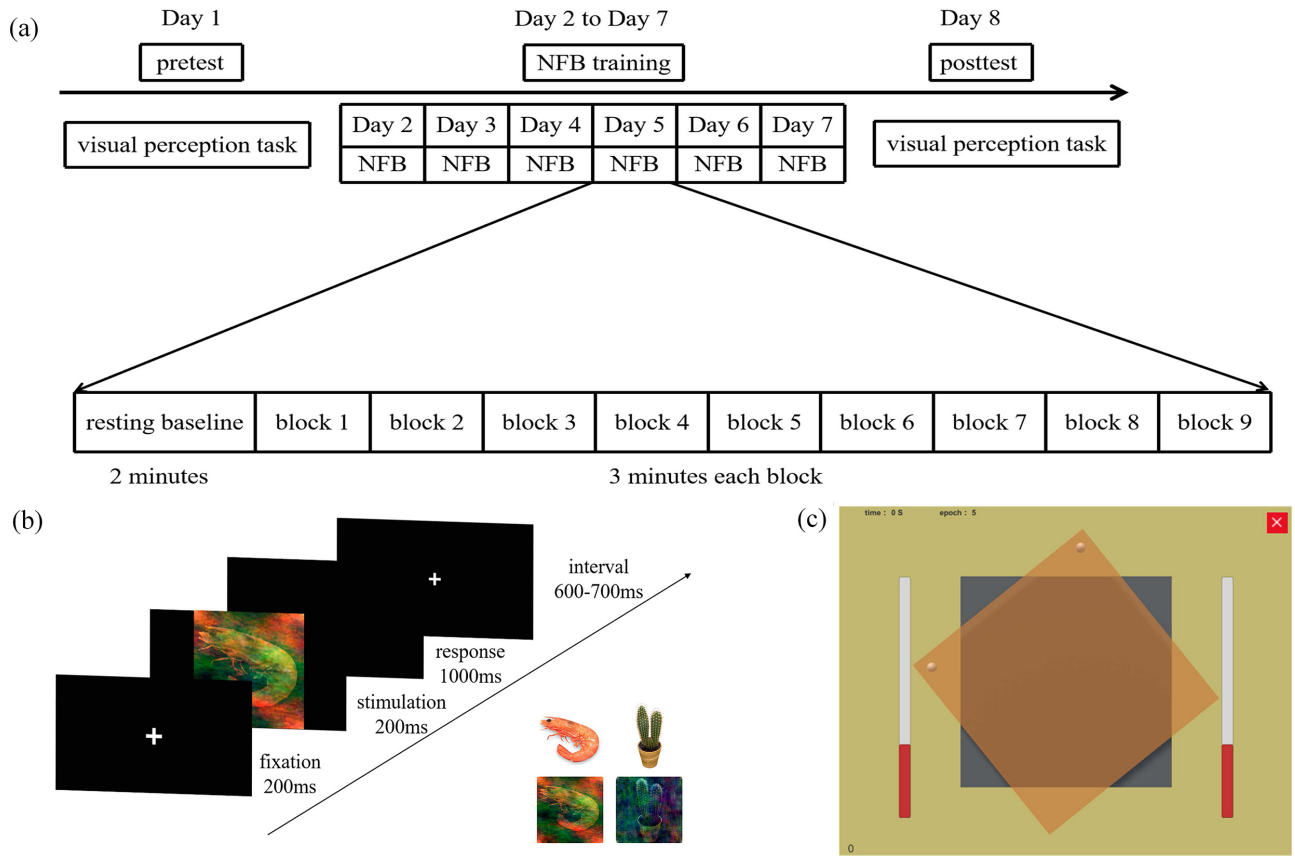

Fig. 1. Overview of the experimental procedure. (a) Overall experimental design. (b) Paradigm for the visual perception task. The images in the lower right corner are example stimuli used in the visual perception task. (c) Visual feedback for neurofeedback (NFB) training.

underwent random transformations. The continuous resting EEG data were segmented into 119 epochs, each with a duration of 2 seconds and a 1-second overlap window. For each epoch, the power spectrum S(f) and the proportion of electromyography (EMG) contamination were calculated as follows:

$$Power_{EMG} = \frac{\sum_{f=40Hz}^{500Hz} S(f) - \sum_{f=48Hz}^{52Hz} S(f)}{\sum_{f=4Hz}^{500Hz} S(f) - \sum_{f=48Hz}^{52Hz} S(f)}$$

The resulting 119 EMG ratios were converted to z-scores. All epochs with z-scores >2 were subsequently excluded to remove those with excessive EMG contamination. The remaining segments were used to calculate the relative gamma and beta power, which served as the baseline for subsequent feedback.

NFB training was conducted with visual feedback, guiding participants through the manipulation of rotating and scaling squares displayed on the screen. Participants sat about one meter from a monitor displaying the feedback interface, which included a rotating orange block over a stationary gray square and two bar graphs. As shown in Fig. 1c, the left bar indicated the real-time training metric, while the right bar displayed the EMG noise level. The left-side bar displayed the real-time training indicator, with the maximum and minimum values corresponding to 120% and 80% of the baseline, respectively. The right-side bar visualized EMG activity ranging from 80% to 120% of baseline. When the EMG activity exceeded 120% of baseline levels, video playback was paused.

During gamma NFB training, the relative gamma power was computed in real-time by applying a Fast Fourier Transform (FFT) with a Hamming window to a 2-second data segment with a 1-second overlap, resulting in a feedback update rate of once per second. There were 9 levels for rotation from maximum (0°) to minimum (−90°). The NFB threshold was set at ±20% of the baseline power. The rotation of the orange square served as the primary visual feedback dimension, with 9 discrete levels spanning from 0° (fully upright, maximum reward state) to −90° (maximum punishment state). When the training indicator exceeded 120% of baseline, the orange square rotated clockwise by one step as visual feedback (reward). Conversely, when the indicator fell below 80% of baseline, the orange square rotated one step counterclockwise linearly as visual feedback (punishment). If the indicator remained within the ±20% baseline range, the orange square remained sta-

Table 1. Baseline demographic characteristics and behavioral measures of the three groups.

Variable	Sham (n = 14)	Gamma (n = 16)	Gamma-beta (n = 14)	Statistics	*p*
Age (years)	21.20 ± 2.81	21.13 ± 1.89	20.79 ± 1.81	$F(2, 41) = 0.140$	0.870
Gender (F/M)	7/7	8/8	7/7	$\chi^2(2) = 0$	1
Baseline ACC	0.78 ± 0.07	0.82 ± 0.06	0.77 ± 0.04	$H(2) = 3.515$	0.173
Baseline RT (ms)	650 ± 75	700 ± 95	640 ± 85	$H(2) = 3.941$	0.139

Values are presented as Mean ± SD. F, female; M, male; ACC, accuracy; RT, reaction time; SD, standard deviation.

tionary. Rotation was clamped at the upper (0°) and lower (−90°) bounds. The size of squares was used as the second degree of freedom, with 9 levels for zoom-in from maximum (100% of screen size) to minimum (20% of screen size). For the gamma-beta group, the size of squares was used to depict beta powers, and the thresholds were also set at ±20% of the baseline beta power. Critically, transitions between feedback levels were not instantaneous. Instead, changes in rotation angle and scale were rendered as smooth 500-ms interpolations using Unity (2021.3 LTS; Unity Technologies, San Francisco, CA, USA). Specifically, the rotation angle was interpolated using Mathf.Lerp, whereas the scale was interpolated using Vector3.Lerp. For both functions, the interpolation parameter t was defined as the elapsed transition time divided by 0.5 s and was constrained to the range of 0–1. Thus, *t* increased linearly from 0 to 1 over each 500-ms transition. This ensured perceptually continuous feedback while preserving the underlying discrete control logic updated once per second.

During each session, participants were instructed to use "mental strategies" (e.g., visual imagery, focused attention) to maximize the alignment of squares (and the size of squares for the gamma-beta group), while minimizing physical movements (e.g., jaw clenching, excessive blinking) to prevent artifacts.

3. Results

Baseline demographic characteristics and behavioral measures are summarized in Table 1. No significant between-group differences were observed in age, gender, baseline accuracy and reaction time (RT) of pretest, indicating that the three groups were comparable before training.

3.1 Analysis of the NFB Training Process

The entire training protocol comprised a total of 54 blocks. Changes in gamma and beta power within the parieto-occipital (PO) region (PO3, POz, PO4, PO5, PO6, O1, Oz, O2) and central region (FC1, FCz, FC2, C1, Cz, C2) across the training period for all 44 participants in the three groups were compared using repeated-measures ANOVA, with groups and time as factors. When the assumption of sphericity was violated, the Greenhouse-Geisser correction was applied, and the corrected degrees of freedom and *p*-values were reported. Both the gamma and gamma-beta groups exhibited significant gamma-band power upregulation within the PO region (repeated-measures ANOVA; gamma group: $F(37.1, 556.5) = 1.641$, $p = 0.011$; $\eta^2 = 0.099$ gamma-beta group: $F(39.8, 516.8) = 1.542$, $p = 0.024$, $\eta^2 = 0.106$), whereas the sham group showed no marked increase in gamma-band power ($F(36.0, 468.5) = 1.340$, $p = 0.094$, $\eta^2 = 0.093$). In contrast, gamma-band power in the central region did not show a notable increase in any of the groups, remaining stable throughout training. Only the gamma-beta group exhibited a significant increase in neural oscillation of beta-band power in the central region ($F(38.6, 501.6) = 2.251$, $p < 0.001$, $\eta^2 = 0.148$), with no significant changes observed in the other groups ($F < 1.3$, $p > 0.05$). Furthermore, none of the three groups showed any significant change in beta-band power in the PO region.

3.2 Analysis of the Pre- and Post-Training Process

The eyes-open resting-state power changes for pre- and post-training EEG recordings are presented in Fig. 2. Statistical analysis revealed no significant differences in baseline power were observed among the three groups for either frequency band in any region (all $p > 0.05$). And significant pre-to-post increases in gamma band power in the PO region were observed in both gamma and gamma-beta groups, whereas no significant change was observed in the sham group (Fig. 2a; repeated-measures ANOVA, $F(2, 41) = 23.208$, $p < 0.001$, $\eta^2 = 0.531$). Only the gamma-beta training group showed a significant increase in beta power in the central cortical region ($F(2, 41) = 7.066$, $p = 0.002$, $\eta^2 = 0.256$). In contrast, no significant changes were observed for gamma power in the central region (Fig. 2b, $F(2, 41) = 1.338$, $p = 0.274$, $\eta^2 = 0.061$) or beta power in the PO region (Fig. 2c, $F(2, 41) = 1.781$, $p = 0.179$, $\eta^2 = 0.080$).

The results for accuracy in the visual perception task assessed pre- and post-training, as well as the respective changes, are presented in Fig. 3. There were no significant differences in baseline (pre-training) accuracy among the three groups (as shown in Table 1). Both gamma and gamma-beta groups exhibited a significant improvement in accuracy compared to the sham group, as shown in Fig. 3a,b. Statistical comparisons for accuracy improvement among the three groups are shown in Fig. 3b. Both training groups demonstrated significantly greater improvements in accuracy than the sham group (Kruskal–Wallis test, $H(2) = 14.300$, $p = 0.001$, $\eta^2 = 0.3$). Post-hoc analyses revealed both the Gamma and gamma-beta groups significantly outperformed the Sham group (both $p < 0.01$), whereas no sig-

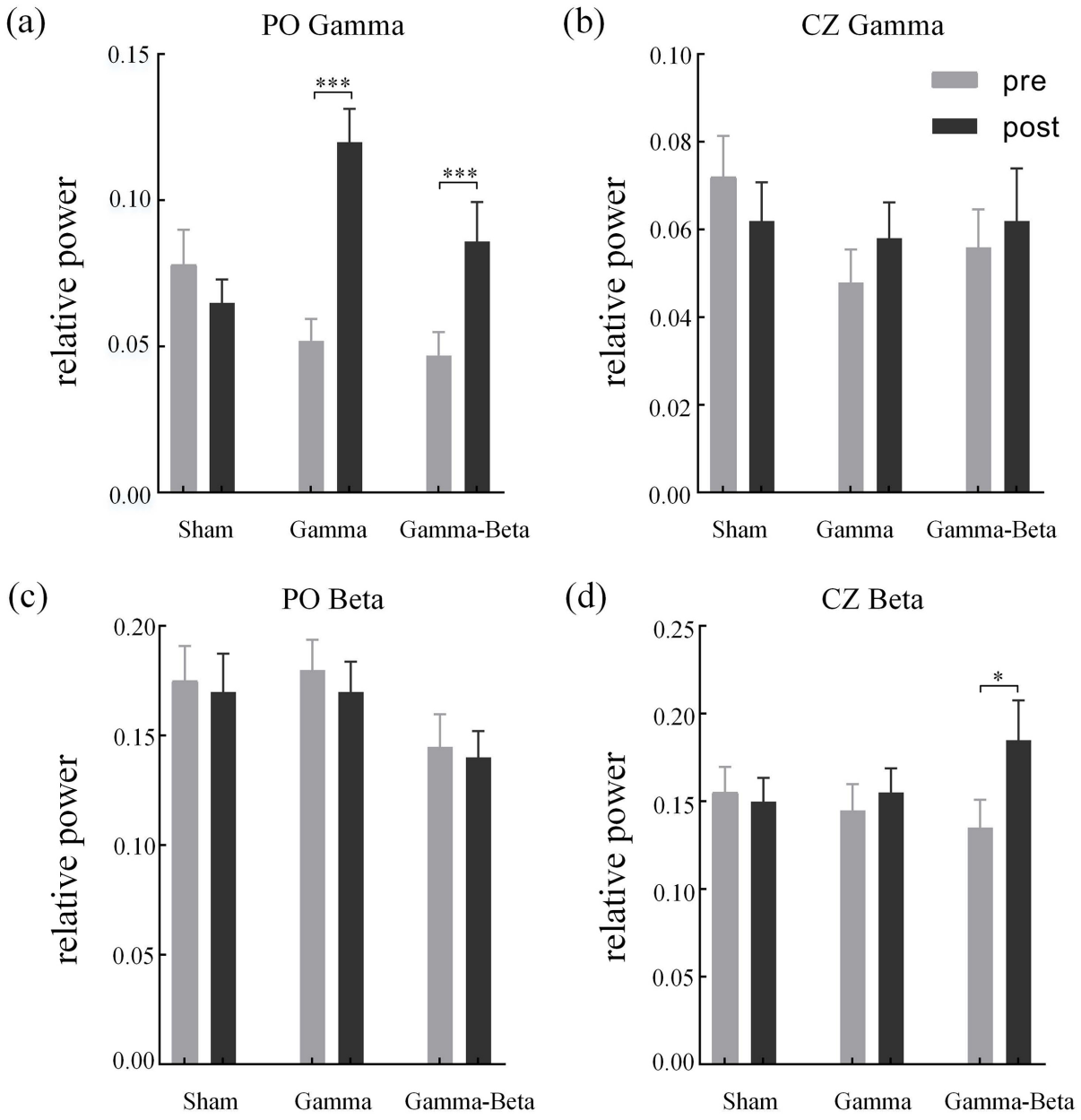

Fig. 2. Changes in resting relative powers before and after NFB training for the three groups, including gamma and beta bands in the parieto-occipital (PO) and central region. (a) PO Gamma, (b) Central Gamma, (c) PO Beta, and (d) Central Beta. Relative power was calculated as the absolute power within gamma or beta band divided by the total spectral power. Gray and black bars represent pre- and post-training, respectively. Error bars indicate the standard error of the mean. * $p < 0.05$, *** $p < 0.001$.

nificant difference in improvement was observed between the two training groups.

The reaction time (RT) during the visual perception task measured in pre- and post-training, as well as the changes, are presented in Fig. 4. There were no significant differences in baseline (pre-training) RT among the three groups (as shown in Table 1). Both the gamma and gamma-beta groups exhibited greater reductions in RT from pre- to post-training than the sham group, as shown in Fig. 4a. Statistical analysis of RT reductions across the three groups is presented in Fig. 4b. Statistically significant inter-group differences were observed for the extent of RT reduction (Kruskal–Wallis test, $H(2) = 6.081$, $p = 0.048$, $\eta^2 = 0.100$). Furthermore, post-hoc comparisons revealed both the gamma and gamma–beta groups showed significantly greater RT reductions than the sham group (both $p < 0.05$), whereas no significant difference in improvement was observed between the two training groups.

To summarize, participants from both training groups showed markedly enhanced behavioral performance in the visual perception task.

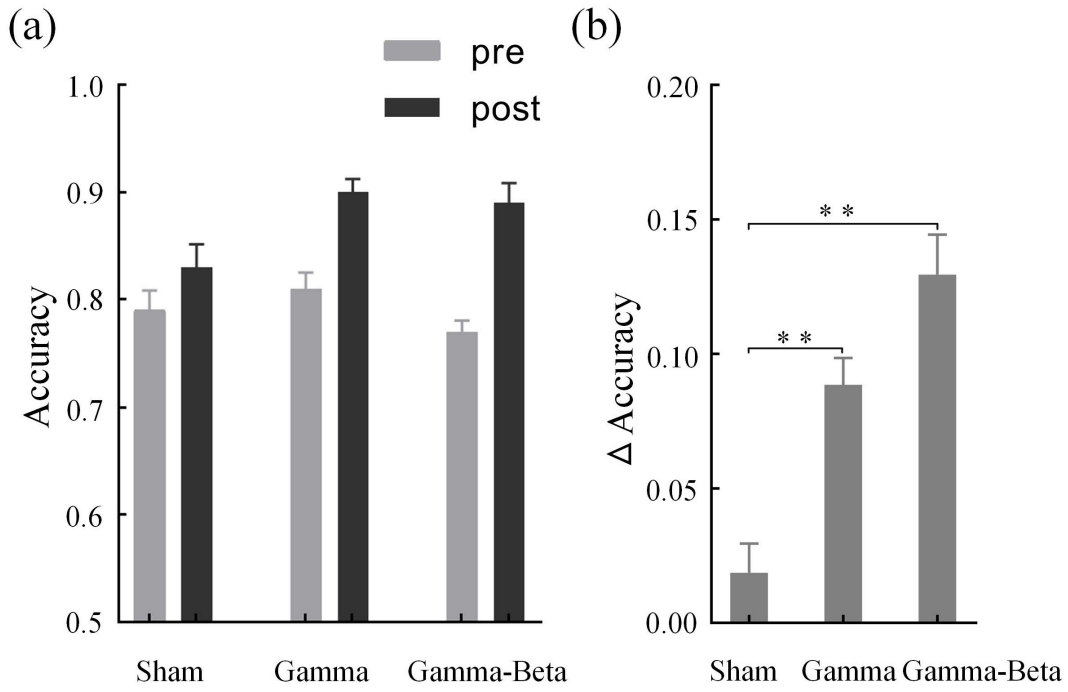

Fig. 3. Changes in visual perception accuracy before and after NFB training. (a) Mean accuracy (±SE) for each group. SE, Standard error. (b) Changes in accuracy (Δ Accuracy = post – pre) across groups. Error bars indicate the standard error of the mean. ** $p < 0.01$.

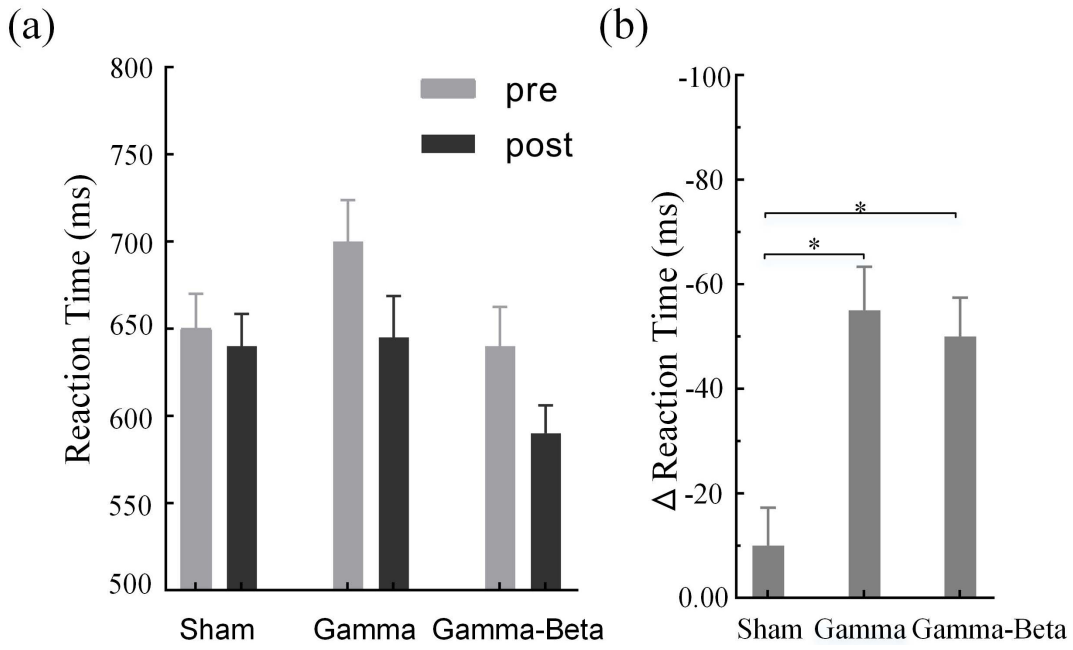

Fig. 4. Changes in visual perception reaction time before and after NFB training. (a) Mean reaction time (ms; ±SE) for each group. (b) Changes in reaction time (Δ RT = post – pre) across groups. Error bars indicate the standard error of the mean. * $p < 0.05$. Negative Δ RT values indicate shorter reaction times after NFB training.

To further clarify whether the behavioral improvements reflected changes in perceptual evidence processing or shifts in decision strategy, we applied the EZ-diffusion model to the RT–accuracy data of visual perception task for each participant and session. The underlying accuracy and RT changes (Pc and mean reaction time (MRT)) used for the EZ-diffusion analysis were consistent with the behavioral results reported above. And the model provided estimates of drift rate (v), boundary separation (a), and non-decision time (t_0).

A one-way ANOVA on the change in drift rate (Δv) revealed a significant group effect, $F(2, 41) = 8.107$, p

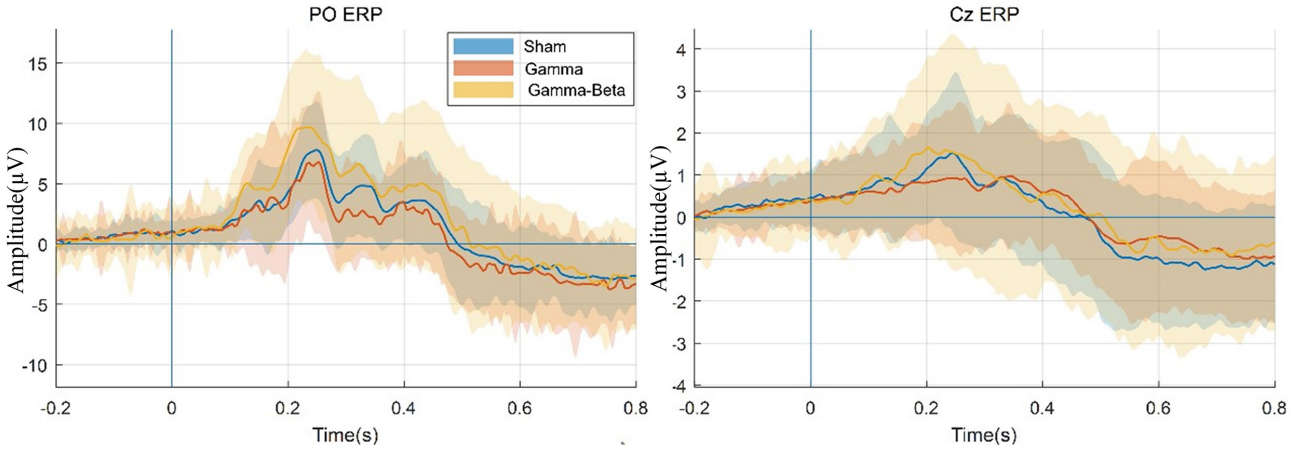

Fig. 5. ERP waveforms of the post-NFB visual perception task of each group. ERP, Event-related potential.

= 0.001, η^2 = 0.288. Both the gamma and gamma–beta groups showed significantly increases (Gamma: $\Delta v = 0.063 \pm 0.009$; gamma–beta: $\Delta v = 0.077 \pm 0.010$; Sham: $\Delta v = 0.026 \pm 0.008$) in drift rate than the sham group ($p = 0.015$ and $p = 0.001$, respectively), whereas the difference between the two active NFB groups was not significant. In contrast, changes in boundary separation (Δa) did not differ reliably between groups, $F(2, 41) = 1.359$, $p = 0.269$, $\eta^2 = 0.064$, and none of the groups showed a significant pre–post change in a (all $p > 0.27$). This suggests that the NFB protocols did not primarily alter decision caution or the response threshold. Non-decision time (Δt_0) showed a significant group effect, $F(2, 41) = 6.159$, $p = 0.005$, $\eta^2 = 0.235$. Both NFB groups exhibited larger reductions (Gamma: $\Delta t_0 = -64.2 \pm 10.1$ ms; gamma–beta: $\Delta t_0 = -52.5 \pm 11.9$ ms; Sham: $\Delta t_0 = -10.4 \pm 11.9$ ms) in t_0 than the sham group ($p = 0.004$ for gamma vs. sham, $p = 0.036$ for gamma–beta vs. sham), whereas the difference between the two active groups was not significant.

Event-related potential (ERP) analyses of the visual perception task administered pre- and post-training were conducted for five components: P1 (80–130 ms, O1, Oz, O2), N1 (150–200 ms, PO3, POz, PO4, PO5, PO6, O1, Oz, O2), P2 (180–250 ms, PO3, POz, PO4, PO5, PO6, O1, Oz, O2), N2 (250–350 ms, FC1, FCz, FC2, C1, Cz, C2), and P3 (300–500 ms, P1, Pz, P2, PO3, POz, PO4). Mean amplitudes were computed within each time window by averaging across the corresponding electrode set. No significant pre- to post-training changes were observed for any component (all $F(2, 41) < 3$, all $p > 0.05$). Post-training ERP waveforms confirmed the successful elicitation of task-related ERP components (Fig. 5). However, due to the considerable variability within groups, no significant differences in ERP components were observed between groups.

Analysis of the event-related time-frequency representation (ERTFR) of the visual perception task using continuous wavelet transform (CWT) is presented in Fig. 6, revealing region-specific spectral perturbations. For each participant, ERTFR power values were averaged across electrodes within the PO and central region, respectively. The grand-average ERTFR maps, collapsed across all participants, groups, and sessions, revealed region-specific spectral perturbation patterns. Notable patterns include beta suppression (13–30 Hz) at 300–500 ms in both the PO and central regions, as well as alpha desynchronization (8–13 Hz) after 550 ms, and theta increase (4–8 Hz) after 500 ms. The gamma rhythm showed an enhancement around 100 ms only in the central region, whereas the beta band displayed significant increases at approximately 100 ms in both regions. Based on the task-related spectral patterns observed in the grand-average maps, two time-frequency regions of interest (TF-ROIs) within the central region were defined prior to any between-group statistical testing: region 1 (beta, 13–30 Hz, 300–500 ms) and region 2 (alpha, 8–13 Hz, 500–700 ms). For each participant, mean power was extracted within each TF-ROI for both pre- and post-training sessions, and pre-to-post difference scores (Δpower) were computed. Between-group differences in Δpower were then assessed using Kruskal–Wallis tests, with false discovery rate (FDR) correction applied across the two TF-ROI comparisons. Significant intergroup differences were observed exclusively within the central cortical region (Kruskal–Wallis test, Region 1: $H(2) = 7.400$, $p = 0.025$, $\eta^2 = 0.132$; Region 2: $H(2) = 6.630$, $p = 0.036$, $\eta^2 = 0.113$). Subsequent pairwise post-hoc comparisons revealed no significant differences between any pair of groups after correction for multiple comparisons.

To examine the neural–behavioral linkage, we extracted subject-wise changes in ERTFR power within the same central-region ROIs and time–frequency windows (region 1: beta 13–30 Hz, 300–500 ms; region 2: alpha: 8–13 Hz, 500–700 ms). For each participant, pre–post differences in mean power (Δbeta, Δalpha) as well as relative changes (Δbeta_rel, Δalpha_rel, normalized by the pre-training magnitude) were computed and correlated with corresponding changes in reaction time and accuracy

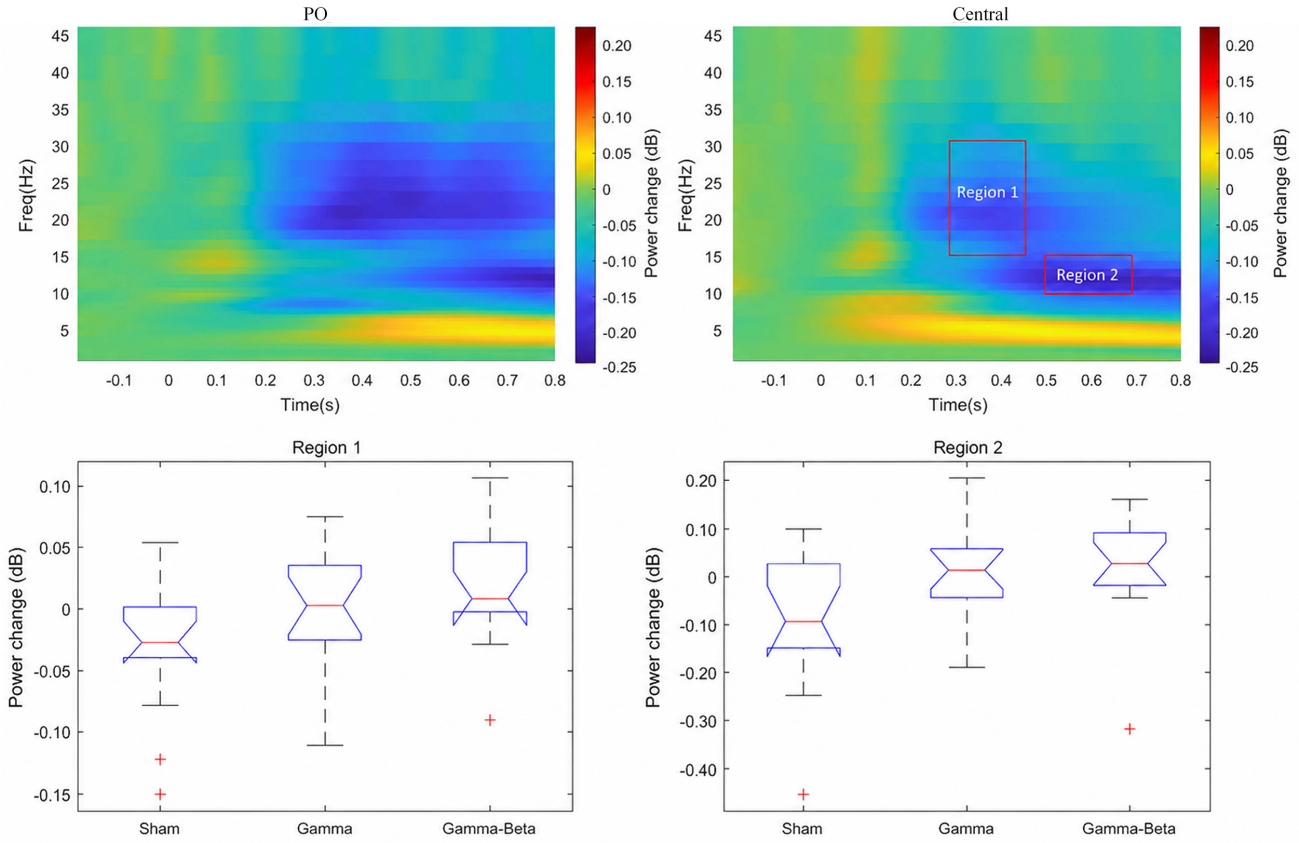

Fig. 6. Event-related time-frequency representation (ERTFR) of the visual perception task. Boxplots were generated using the notched boxplot function in MATLAB. Center lines indicate medians; box limits indicate the 25th and 75th percentiles; whiskers extend to the most extreme data points not considered outliers; crosses denote outliers. Notches represent the approximate 95% confidence interval of the median. In cases of small sample size or skewed distributions, this confidence interval may extend beyond the interquartile range, which can cause the notches to visually narrow or extend towards the box limits, as observed for some groups.

(ΔRT, ΔAccuracy (ΔACC), and their relative changes) in the gamma and gamma–beta groups. Across the gamma and gamma–beta groups, individual pre–post changes in central beta and alpha power showed no robust correlations with improvements in reaction time or accuracy. For absolute changes, all neural–behavior correlations were small and non-significant (Δbeta vs. ΔRT: r = –0.01, p = 0.95; Δalpha vs. ΔRT: r = 0.01, p = 0.95; Δbeta vs. ΔACC: r = –0.34, p = 0.06; Δalpha vs. ΔACC: r = –0.35, p = 0.06). Using relative changes, we observed at most a modest association between alpha modulation and RT improvement at the uncorrected level (r = 0.40, p = 0.028). However, this association did not remain significant after non-parametric correlation analysis or FDR correction for multiple comparisons and was therefore not interpreted as a robust effect.

4. Discussion

In this study, we systematically investigated the effects of gamma and gamma-beta NFB training on visual perception abilities in healthy adults. During the training process, both groups demonstrated selective enhancement of gamma (gamma group) or combined gamma/beta (gamma-beta group) oscillations. Moreover, the pre- and post-training resting-state EEGs replicated these observations, demonstrating clear region-specific enhancement of targeted frequency bands. At the behavioral level, both gamma and gamma-beta NFB groups showed improved reaction time and accuracy on the visual perception task relative to baseline, whereas the sham group showed no such changes. Although the gamma group exhibited numerically larger reductions in reaction time and the gamma-beta group showed descriptively greater gains in accuracy, these between-group differences did not reach statistical significance after correction for multiple comparisons. Accordingly, we refrain from making strong claims about a qualitative dissociation in behavioral profiles between the two active NFB protocols. Instead, we interpret the observed patterns as tentative trends that require replication in larger samples. Overall, the present findings provide converging evidence that gamma- and beta-rhythm NFB can modulate both oscillatory activity and visual detection performance in a frequency- and region-sensitive manner.

Our findings provide compelling evidence for spectral- and regional-specific effects of NFB training.

Specifically, gamma-band power increased significantly in the PO regions for both gamma and gamma-beta groups, while central beta activity increased exclusively in the gamma-beta group. Furthermore, these results are consistent with previous studies demonstrating gamma rhythm modulation within visual cortical areas [24,27], and with beta-rhythm improving visual information processing and reducing visual reaction times in task performance [37,39]. Importantly, the spatial dissociation between posterior gamma and central beta changes suggests the two protocols may engage partly distinct functional networks, even though their behavioral consequences were only partially differentiated at the group level.

The behavioral improvements did not differ significantly between the two active groups. However, the descriptive pattern of faster responses in the gamma group, and higher accuracy in the gamma–beta group, is broadly consistent with the notion that gamma and beta rhythms may serve complementary, partly distinct roles in the cognitive processes underlying visual perception. Complementing the standard RT and accuracy analyses, the EZ-diffusion modeling provided a more fine-grained view of the underlying decision processes. In line with the overall behavioral pattern, neurofeedback primarily modulated drift rate and non-decision time, whereas boundary separation remained relatively stable across groups. Although the simplifying assumptions of the EZ model and the modest sample size warrant caution, these results tentatively suggest that gamma- and beta-rhythm neurofeedback enhance perceptual evidence accumulation and speed non-decision processes rather than merely shifting decision thresholds. Prior work has linked beta rhythms to general cortical activation and arousal states such as alertness, attention, excitation, and cognitive engagement [47,48]. However, beyond general arousal, recent theoretical frameworks suggest more specific mechanistic roles. Gamma rhythm primarily contributes to localized neural processing, where it promotes synchronous neural firing which is essential for rapid information processing [49,50]. Gamma oscillations are fundamentally linked to local cortical computation and the "binding problem". According to the Communication through Coherence (CTC) hypothesis, gamma synchronization ensures that neuronal groups fire within a precise temporal window, maximizing their impact on downstream targets [1,51]. In our study, the enhanced posterior gamma power likely facilitated the rapid binding of visual features into coherent percepts, thereby accelerating the accumulation of sensory evidence required for the detection decision. This aligns with our observation of numerically shorter response times in the gamma group. In contrast, beta-band activity—particularly over central and frontal regions—is increasingly associated with top-down predictive processing and the "maintenance of the status quo" [52,53]. In the context of our animal detection task, enhanced beta power may support the maintenance of the cognitive rule or "search template" in working memory and facilitate the stabilization of sensory representations against noise [52,53,54,55]. By strengthening these top-down priors, beta enhancement effectively lowers the neural noise floor, supporting more reliable and accurate decision-making rather than merely faster processing [54,55]. However, we emphasize that our behavioral data does not allow us to definitively dissociate these mechanisms between the two NFB protocols. Instead, they are best viewed as plausible mechanistic interpretations grounded in the broader literature.

We also considered the possibility of synergistic interactions between gamma and beta rhythms, but did not find evidence for supra-additive neural effects (i.e., neural changes in the gamma–beta group exceeding the summed changes of single-band training). However, the manner in which the gamma–beta protocol produced robust neural modulation of both posterior gamma and central beta bands, together with its numerically improved accuracy, is compatible with a functional complementarity account. When both gamma and beta rhythms were simultaneously trained, bottom-up enhancement of sensory encoding (gamma) may operate in concert with top-down stabilization and control (beta), potentially yielding a more balanced speed–accuracy profile than either rhythm alone [56]. Given the lack of statistically significant behavioral differences between the two active groups, this interpretation should be regarded as speculative and invites further work designed to more directly probe gamma–beta interactions.

Despite the robust behavioral improvements, no significant training effect was observed in ERP components. This is likely attributable to reduced statistical power due to the high intra-group variability in ERP waveforms. Nevertheless, our null finding is consistent with previous literature, indicating the ERP amplitudes and latencies may be less sensitive to subtle neural modulation achieved by short-term NFB training [57]. However, the ERTFR analyses revealed that NFB training induced meaningful changes, and in particular increased beta suppression and alpha desynchronization in the central cortical region. This highlights the sensitivity of time-frequency analyses compared to ERPs in detecting training-induced neural plasticity. Furthermore, the significant ERTFR effects indicate that beta and alpha rhythms, even if not the explicit targets of all groups, are responsive to training and may underlie improved perceptual performance via top-down attention or cognitive control mechanisms.

To further probe the mechanistic link between the observed neural modulation and behavioral gains, we examined subject-wise correlations between changes in central ERTFR power and improvements in reaction time or accuracy. Contrary to the robust group-level effects, we found no strong linear correlations between the magnitude of individual neural changes and behavioral outcomes. Taken together, these findings suggest that, while neurofeedback robustly modulated oscillatory dynamics and improved vi-

sual detection performance at the group level, the present dataset does not provide strong evidence for a tight linear coupling between the magnitude of ERTFR changes and individual behavioral gains. This pattern is compatible with the idea that oscillatory plasticity constitutes a necessary but not solely sufficient condition for behavioral improvement, and that additional factors—such as strategy use, baseline efficiency, or non-neural sources of variability—may also play an important role in shaping individual outcomes.

Several limitations of the present study should be acknowledged. First, the sample size was modest, which may have limited the detection of smaller effects and reduced the generalizability of the findings. Second, we did not include follow-up sessions, thus preventing assessment of the long-term retention of NFB-induced changes in oscillatory activity and behavior. Third, individual differences in NFB learning strategies and regulation efficacy were not explicitly modeled, which may account for part of the observed variability across participants [35]. Relatedly, our neural–behavioral correlation analyses were necessarily exploratory and underpowered, and the absence of strong subject-wise coupling should therefore be interpreted with caution. Finally, while we employed EZ-diffusion modeling to decompose the decision components, this simplified approach relies on summary statistics (mean RT and variance) rather than full distribution fitting. The number of trials and task structure in our study were optimized for NFB rather than for complex cognitive modeling, thereby constraining the application of full hierarchical Bayesian drift diffusion model (DDM) approaches. Future studies should employ designs with larger trial counts to address this. Furthermore, given the modest sample sizes (n = 14–16 per group), effect-size estimates and individual-difference analyses should be interpreted cautiously, and the mechanistic interpretations we offer are intended as tentative rather than definitive.

We explicitly acknowledge this limitation and note the importance of future studies incorporating experimental manipulations specifically tailored to DDM/signal detection theory (SDT) (e.g., graded stimulus difficulty, asymmetric prior probabilities, or payoff structures). These should allow a more precise characterization of how gamma- and beta-rhythm NFB influence perceptual evidence processing, decision thresholds, and response tendencies within the visual system.

5. Conclusions

This study demonstrates that neurofeedback (NFB) can effectively enhance visual perception through the rhythm-specific modulation of cortical oscillations. While both gamma and gamma–beta training improved detection performance alongside increased parieto-occipital gamma activity—consistent with gamma's role in sensory encoding—the dual-band protocol uniquely recruited a top-down mechanism characterized by central beta upregulation and modified post-stimulus suppression. The observed spectral and regional specificity, where gamma modulations were restricted to posterior sites and beta effects emerged only centrally in the dual-band group, underscores the dissociable functional roles of these rhythms in bottom-up and top-down visual processing.

Using a rigorous double-blind, sham-controlled framework, our findings highlight NFB as a viable tool for probing the causal contributions of neural rhythms to perception. However, the modest sample size and the observed discrepancy between group-level effects and individual neural–behavioral coupling necessitate a cautious interpretation of these specific mechanisms. Future research utilizing larger cohorts and designs tailored for hierarchical cognitive modeling remains essential to clarify how multi-band neurofeedback reshapes oscillatory dynamics and to determine the extent to which such plasticity can be reliably harnessed for targeted cognitive enhancement.

Availability of Data and Materials

The data generated and analyzed during the current study are not publicly available for ethical reasons, but the de-identified data are available from the corresponding authors on reasonable request.

Author Contributions

All authors participated in the conception and discussion of the study design and contributed to the development of the overall research plan. LW and HC conceived and designed the study and were responsible for data acquisition and analysis. LW drafted the manuscript. YW, ZD, HC and XL provided critical revision of the manuscript for important intellectual content, guidance, and oversight. XL secured funding. All authors contributed to editorial changes in the manuscript. All authors reviewed and approved the final version of the manuscript. All authors have participated sufficiently in the work and agreed to be accountable for all aspects of the work.

Ethics Approval and Consent to Participate

This study was performed in accordance with the Declaration of Helsinki and the CONSORT guidelines. This study was approved by the ethics committee of Beijing Normal University (Ethic Approval Number: CNL_A_0010_003). All participants were provided with detailed information regarding the study. All participants provided written informed consent.

Acknowledgment

We gratefully acknowledge all participants for their participation.

Funding

This research was funded by the Science and Technology Innovation 2030 (STI2030) Major Projects under Grant No.2021ZD0204300.

Conflicts of Interest

The authors declare no conflicts of interest.

Supplementary Material

Supplementary material associated with this article can be found, in the online version, at https://doi.org/10.31083/JIN46741.

References

[1] Fries P. Rhythms for Cognition: Communication through Coherence. Neuron. 2015; 88: 220–235. https://doi.org/10.1016/j.neuron.2015.09.034

[2] Engel AK, Fries P, Singer W. Dynamic predictions: oscillations and synchrony in top-down processing. Nature Reviews. Neuroscience. 2001; 2: 704–716. https://doi.org/10.1038/35094565

[3] Marzbani H, Marateb HR, Mansourian M. Methodological Note: Neurofeedback: A Comprehensive Review on System Design, Methodology and Clinical Applications. Basic and Clinical Neuroscience. 2016; 7: 143–158. https://doi.org/10.15412/J.BCN.03070208

[4] Barry RJ, Clarke AR, Johnstone SJ, Magee CA, Rushby JA. EEG differences between eyes-closed and eyes-open resting conditions. Clinical Neurophysiology. 2007; 118: 2765–2773. https://doi.org/10.1016/j.clinph.2007.07.028

[5] Ward LM, Doesburg SM, Kitajo K, MacLean SE, Roggeveen AB. Neural synchrony in stochastic resonance, attention, and consciousness. Canadian Journal of Experimental Psychology. 2006; 60: 319–326. https://doi.org/10.1037/cjep2006029

[6] Gruenwald J, Sieghartsleitner S, Kapeller C, Scharinger J, Kamada K, Brunner P, et al. Characterization of High-Gamma Activity in Electrocorticographic Signals. Frontiers in Neuroscience. 2023; 17: 1206120. https://doi.org/10.3389/fnins.2023.1206120

[7] Berger B, Griesmayr B, Minarik T, Biel AL, Pinal D, Sterr A, et al. Dynamic regulation of interregional cortical communication by slow brain oscillations during working memory. Nature Communications. 2019; 10: 4242. https://doi.org/10.1038/s41467-019-12057-0

[8] Shirhatti V, Ravishankar P, Ray S. Gamma oscillations in primate primary visual cortex are severely attenuated by small stimulus discontinuities. PLoS Biology. 2022; 20: e3001666. https://doi.org/10.1371/journal.pbio.3001666

[9] Wittevrongel B, Khachatryan E, Carrette E, Boon P, Meurs A, Van Roost D, et al. High-gamma oscillations precede visual steady-state responses: A human electrocorticography study. Human Brain Mapping. 2020; 41: 5341–5355. https://doi.org/10.1002/hbm.25196

[10] Bonnefond M, Kastner S, Jensen O. Communication between Brain Areas Based on Nested Oscillations. eneuro. 2017; 4: ENEURO.0153-16.2017. https://doi.org/10.1523/ENEURO.0153-16.2017

[11] Herrmann CS, Strüber D, Helfrich RF, Engel AK. EEG oscillations: From correlation to causality. International Journal of Psychophysiology. 2016; 103: 12–21. https://doi.org/10.1016/j.ijpsycho.2015.02.003

[12] Cabral-Calderin Y, Wilke M. Probing the Link Between Perception and Oscillations: Lessons from Transcranial Alternating Current Stimulation. The Neuroscientist. 2020; 26: 57–73. https://doi.org/10.1177/1073858419828646

[13] Elyamany O, Leicht G, Herrmann CS, Mulert C. Transcranial alternating current stimulation (tACS): from basic mechanisms towards first applications in psychiatry. European Archives of Psychiatry and Clinical Neuroscience. 2021; 271: 135–156. https://doi.org/10.1007/s00406-020-01209-9

[14] Reato D, Rahman A, Bikson M, Parra LC. Effects of weak transcranial alternating current stimulation on brain activity-a review of known mechanisms from animal studies. Frontiers in Human Neuroscience. 2013; 7: 687. https://doi.org/10.3389/fnhum.2013.00687

[15] Vosskuhl J, Strüber D, Herrmann CS. Non-invasive Brain Stimulation: A Paradigm Shift in Understanding Brain Oscillations. Frontiers in Human Neuroscience. 2018; 12: 211. https://doi.org/10.3389/fnhum.2018.00211

[16] Fertonani A, Miniussi C. Transcranial Electrical Stimulation: What We Know and Do Not Know About Mechanisms. The Neuroscientist. 2017; 23: 109–123. https://doi.org/10.1177/1073858416631966

[17] Fertonani A, Ferrari C, Miniussi C. What do you feel if I apply transcranial electric stimulation? Safety, sensations and secondary induced effects. Clinical Neurophysiology. 2015; 126: 2181–2188. https://doi.org/10.1016/j.clinph.2015.03.015

[18] Bjekić J, Živanović M, Stanković M, Paunović D, Konstantinović U, Filipović SR. The subjective experience of transcranial electrical stimulation: a within-subject comparison of tolerability and side effects between tDCS, tACS, and otDCS. Frontiers in Human Neuroscience. 2024; 18: 1468538. https://doi.org/10.3389/fnhum.2024.1468538

[19] Rossi S, Hallett M, Rossini PM, Pascual-Leone A. Safety, ethical considerations, and application guidelines for the use of transcranial magnetic stimulation in clinical practice and research. Clinical Neurophysiology. 2009; 120: 2008–2039. https://doi.org/10.1016/j.clinph.2009.08.016

[20] Sulzer J, Papageorgiou TD, Goebel R, Hendler T. Neurofeedback: new territories and neurocognitive mechanisms of endogenous neuromodulation. Philosophical Transactions of the Royal Society of London. Series B, Biological Sciences. 2024; 379: 20230081. https://doi.org/10.1098/rstb.2023.0081

[21] Sitaram R, Ros T, Stoeckel L, Haller S, Scharnowski F, Lewis-Peacock J, et al. Closed-loop brain training: the science of neurofeedback. Nature Reviews. Neuroscience. 2017; 18: 86–100. https://doi.org/10.1038/nrn.2016.164

[22] Ros T, J Baars B, Lanius RA, Vuilleumier P. Tuning pathological brain oscillations with neurofeedback: a systems neuroscience framework. Frontiers in Human Neuroscience. 2014; 8: 1008. https://doi.org/10.3389/fnhum.2014.01008

[23] Keizer AW, Verment RS, Hommel B. Enhancing cognitive control through neurofeedback: a role of gamma-band activity in managing episodic retrieval. NeuroImage. 2010; 49: 3404–3413. https://doi.org/10.1016/j.neuroimage.2009.11.023

[24] Salari N, Büchel C, Rose M. Neurofeedback training of gamma band oscillations improves perceptual processing. Experimental Brain Research. 2014; 232: 3353–3361. https://doi.org/10.1007/s00221-014-4023-9

[25] Enriquez-Geppert S, Huster RJ, Herrmann CS. EEG-Neurofeedback as a Tool to Modulate Cognition and Behavior: A Review Tutorial. Frontiers in Human Neuroscience. 2017; 11: 51. https://doi.org/10.3389/fnhum.2017.00051

[26] Chang M, Suzuki S, Kurose T, Ibaraki T. Pretraining alpha rhythm enhancement by neurofeedback facilitates short-term perceptual learning and improves visual acuity by facilitated consolidation. Frontiers in Neuroergonomics. 2024; 5: 1399578. https://doi.org/10.3389/fnrgo.2024.1399578

[27] Merkel N, Wibral M, Bland G, Singer W. Endogenously generated gamma-band oscillations in early visual cortex: A neuro-

feedback study. Human Brain Mapping. 2018; 39: 3487–3502. https://doi.org/10.1002/hbm.24189
[28] Gruzelier JH. EEG-neurofeedback for optimising performance. III: a review of methodological and theoretical considerations. Neuroscience and Biobehavioral Reviews. 2014; 44: 159–182. https://doi.org/10.1016/j.neubiorev.2014.03.015
[29] Shibata K, Watanabe T, Sasaki Y, Kawato M. Perceptual learning incepted by decoded fMRI neurofeedback without stimulus presentation. Science. 2011; 334: 1413–1415. https://doi.org/10.1126/science.1212003
[30] deBettencourt MT, Cohen JD, Lee RF, Norman KA, Turk-Browne NB. Closed-loop training of attention with real-time brain imaging. Nature Neuroscience. 2015; 18: 470–475. https://doi.org/10.1038/nn.3940
[31] Sitaram R, Lee S, Ruiz S, Rana M, Veit R, Birbaumer N. Real-time support vector classification and feedback of multiple emotional brain states. NeuroImage. 2011; 56: 753–765. https://doi.org/10.1016/j.neuroimage.2010.08.007
[32] Niazi AM, van den Broek PLC, Klanke S, Barth M, Poel M, Desain P, et al. Online decoding of object-based attention using real-time fMRI. The European Journal of Neuroscience. 2014; 39: 319–329. https://doi.org/10.1111/ejn.12405
[33] Mayer K, Wyckoff SN, Fallgatter AJ, Ehlis AC, Strehl U. Neurofeedback as a nonpharmacological treatment for adults with attention-deficit/hyperactivity disorder (ADHD): study protocol for a randomized controlled trial. Trials. 2015; 16: 174. https://doi.org/10.1186/s13063-015-0683-4
[34] Kim DY, Yoo SS, Tegethoff M, Meinlschmidt G, Lee JH. The inclusion of functional connectivity information into fMRI-based neurofeedback improves its efficacy in the reduction of cigarette cravings. Journal of Cognitive Neuroscience. 2015; 27: 1552–1572. https://doi.org/10.1162/jocn_a_00802
[35] Diotaiuti P, Corrado S, Tosti B, Spica G, Di Libero T, D'Oliveira A, et al. Evaluating the effectiveness of neurofeedback in chronic pain management: a narrative review. Frontiers in Psychology. 2024; 15: 1369487. https://doi.org/10.3389/fpsyg.2024.1369487
[36] Keizer AW, Verschoor M, Verment RS, Hommel B. The effect of gamma enhancing neurofeedback on the control of feature bindings and intelligence measures. International Journal of Psychophysiology. 2010; 75: 25–32. https://doi.org/10.1016/j.ijpsycho.2009.10.011
[37] Maszczyk A, Dobrakowski P, Nitychoruk M, Żak M, Kowalczyk M, Toborek M. The Effect of Neurofeedback Training on the Visual Processing Efficiency in Judo Athletes. Journal of Human Kinetics. 2020; 71: 219–227. https://doi.org/10.2478/hukin-2019-0097
[38] Mikicin M. Psychological Evaluation of Attention Indices and Directed Visual Perception Using Neurofeedback Training. Advances in Cognitive Psychology. 2021; 17: 230–238. https://doi.org/10.5709/acp-0332-9
[39] Prończuk M, Trybek G, Terbalyan A, Markowski J, Pilch J, Krzysztofik M, et al. The Effects of EEG Biofeedback Training on Visual Reaction Time in Judo Athletes. Journal of Human Kinetics. 2023; 89: 247–258. https://doi.org/10.5114/jhk/174272
[40] Kober SE, Witte M, Neuper C, Wood G. Specific or nonspecific? Evaluation of band, baseline, and cognitive specificity of sensorimotor rhythm- and gamma-based neurofeedback. International Journal of Psychophysiology. 2017; 120: 1–13. https://doi.org/10.1016/j.ijpsycho.2017.06.005
[41] Dessy E, Mairesse O, van Puyvelde M, Cortoos A, Neyt X, Pattyn N. Train Your Brain? Can We Really Selectively Train Specific EEG Frequencies With Neurofeedback Training. Frontiers in Human Neuroscience. 2020; 14: 22. https://doi.org/10.3389/fnhum.2020.00022
[42] White DJ, Congedo M, Ciorciari J. Source-based neurofeedback methods using EEG recordings: training altered brain activity in a functional brain source derived from blind source separation. Frontiers in Behavioral Neuroscience. 2014; 8: 373. https://doi.org/10.3389/fnbeh.2014.00373
[43] Zoefel B, Huster RJ, Herrmann CS. Neurofeedback training of the upper alpha frequency band in EEG improves cognitive performance. NeuroImage. 2011; 54: 1427–1431. https://doi.org/10.1016/j.neuroimage.2010.08.078
[44] Corlier J, Rimsky-Robert D, Valderrama M, Lehongre K, Adam C, Clémenceau S, et al. Self-induced intracerebral gamma oscillations in the human cortex. Brain. 2016; 139: 3084–3091. https://doi.org/10.1093/brain/aww246
[45] Donner TH, Siegel M. A framework for local cortical oscillation patterns. Trends in Cognitive Sciences. 2011; 15: 191–199. https://doi.org/10.1016/j.tics.2011.03.007
[46] Ni L, Liu Y, Yu W, Fu X. The China Image Set (CIS): A New Set of 551 Colored Photos With Chinese Norms for 12 Psycholinguistic Variables. Frontiers in Psychology. 2019; 10: 2631. https://doi.org/10.3389/fpsyg.2019.02631
[47] Kamiński J, Brzezicka A, Gola M, Wróbel A. β band oscillations engagement in human alertness process. International Journal of Psychophysiology: Official Journal of the International Organization of Psychophysiology. 2012; 85: 125–128. https://doi.org/10.1016/j.ijpsycho.2011.11.006
[48] Gola M, Kamiński J, Brzezicka A, Wróbel A. β band oscillations as a correlate of alertness–changes in aging. International Journal of Psychophysiology: Official Journal of the International Organization of Psychophysiology. 2012; 85: 62–67. https://doi.org/10.1016/j.ijpsycho.2011.09.001
[49] Fries P. Neuronal gamma-band synchronization as a fundamental process in cortical computation. Annual Review of Neuroscience. 2009; 32: 209–224. https://doi.org/10.1146/annurev.neuro.051508.135603
[50] Buzsáki G, Wang XJ. Mechanisms of gamma oscillations. Annual Review of Neuroscience. 2012; 35: 203–225. https://doi.org/10.1146/annurev-neuro-062111-150444
[51] Fries P. A mechanism for cognitive dynamics: neuronal communication through neuronal coherence. Trends in Cognitive Sciences. 2005; 9: 474–480. https://doi.org/10.1016/j.tics.2005.08.011
[52] Engel AK, Fries P. Beta-band oscillations–signalling the status quo? Current Opinion in Neurobiology. 2010; 20: 156–165. https://doi.org/10.1016/j.conb.2010.02.015
[53] Spitzer B, Haegens S. Beyond the Status Quo: A Role for Beta Oscillations in Endogenous Content (Re)Activation. eneuro. 2017; 4: ENEURO.0170-17.2017. https://doi.org/10.1523/ENEURO.0170-17.2017
[54] Arnal LH. Predicting "When" Using the Motor System's Beta-Band Oscillations. Frontiers in Human Neuroscience. 2012; 6: 225. https://doi.org/10.3389/fnhum.2012.00225
[55] Schmidt R, Herrojo Ruiz M, Kilavik BE, Lundqvist M, Starr PA, Aron AR. Beta Oscillations in Working Memory, Executive Control of Movement and Thought, and Sensorimotor Function. The Journal of Neuroscience. 2019; 39: 8231–8238. https://doi.org/10.1523/JNEUROSCI.1163-19.2019
[56] Lundqvist M, Miller EK, Nordmark J, Liljefors J, Herman P. Beta: bursts of cognition. Trends in Cognitive Sciences. 2024; 28: 662–676. https://doi.org/10.1016/j.tics.2024.03.010
[57] Pei G, Yang R, Shi Z, Guo G, Wang S, Liu M, et al. Enhancing Working Memory Based on Mismatch Negativity Neurofeedback in Subjective Cognitive Decline Patients: A Preliminary Study. Frontiers in Aging Neuroscience. 2020; 12: 263. https://doi.org/10.3389/fnagi.2020.00263